ARTICLE

Silk fibroin peptide suppresses proliferation and induces apoptosis and cell cycle arrest in human lung cancer cells

Mei-sa Wang[1], Yi-bo Du[1], Hui-ming Huang[2], Zhong-ling Zhu[1], Shuang-shuang Du[1], Shao-yong Chen[2], Hong-ping Zhao[2] and Zhao Yan[1]

Silkworm cocoon was recorded to cure carbuncle in the Compendium of Materia Medica. Previous studies have demonstrated that the supplemental silk protein sericin exhibits anticancer activity. In the present study, we investigated the effects of silk fibroin peptide (SFP) extracted from silkworm cocoons against human lung cancer cells in vitro and in vivo and its possible anticancer mechanisms. SFP that we prepared had high content of glycine (~ 30%) and showed a molecular weight of ~ 10 kDa. Intragastric administration of SFP (30 g/kg/d) for 14 days did not affect the weights, vital signs, routine blood indices, and blood biochemical parameters in mice. MTT assay showed that SFP dose-dependently inhibited the growth of human lung cancer A549 and H460 cells in vitro with IC_{50} values of 9.921 and 9.083 mg/mL, respectively. SFP also dose-dependently suppressed the clonogenic activity of the two cell lines. In lung cancer H460 xenograft mice, intraperitoneal injection of SFP (200 or 500 mg/kg/d) for 40 days significantly suppressed the tumor growth, but did not induce significant changes in the body weight. We further examined the effects of SFP on cell cycle and apoptosis in H460 cells using flow cytometry, which revealed that SFP-induced cell cycle arrest at the S phase, and then promoted cell apoptosis. We demonstrated that SFP (20−50 mg/mL) dose-dependently downregulates Bcl-2 protein expression and upregulates Bax protein in H460 cells during cell apoptosis. The results suggest that SFP should be studied further as a novel therapeutic agent for the treatment of lung cancer.

INTRODUCTION

Lung cancer has been the leading cancer diagnosis and the most common cause of cancer death in China for many years [1]. Recently, the reported lung cancer incidence and mortality rates have increased in both men and women [2].

Currently, the gold standard treatment for lung cancer is chemotherapy based on platinum agents, such as cisplatin, carboplatin, and oxaliplatin, usually in combination with other agents, such as paclitaxel and etoposide [3]. Traditional chemotherapy drugs have the common drawback of high toxicity. Thus, efforts have focused on the development of novel drugs for lung cancer treatment with enhanced efficacy and reduced toxicity. In particular, compounds extracted from natural biological materials have been of great interest [4, 5].

Silk cocoons spun by silkworm larvae are composed of two major proteins, fibroin and sericin [6], and are widely used in textiles, medical engineering, and industrial applications [7–11]. In the Compendium of Materia Medica, silk cocoons are reported to cure carbuncles. Previous studies demonstrated that the supplemental silk protein sericin can suppress colon tumorigenesis in 1,2-dimethylhydrazine-treated mice by reducing oxidative stress and cell proliferation [12], and it also decreases human colorectal cancer SW480 cell viability in vitro [13]. In addition, the silk protein fibroin was used as a coating in a drug-loaded delivery system for

the controlled release of various drugs [14]. For example, silk fibroin (SF)-coated liposomal emodin showed higher efficacy against breast cancer cells compared with the uncoated liposomal emodin due to increased retention of emodin in the presence of SF [15]. In this study, we applied a normal degumming process to remove the outer sericin and to obtain the silk fibroin peptide (SFP) with additional hydrolysis and enzymatic degradation methods.

Previous studies demonstrated that peptides derived from natural sources can inhibit the proliferation of lung cancer cells. Prateep A et al. [16] reported that peptides extracted from *Lentinus squarrosulus* induce apoptosis in human lung cancer cells. A *Ganoderma lucidum* polysaccharide peptide inhibits the growth of vascular endothelial cells and the induction of vascular endothelial growth factor in human lung cancer cells [17]. A novel synthetic peptide derived from *Conus californicus* venom could induce apoptosis in human lung cancer cell lines [18]. In addition, the soybean-derived peptide lunasin inhibits non-small cell lung cancer cell proliferation by suppressing phosphorylation of the retinoblastoma protein [19]. We focused on the antitumor effect of SFP on lung cancer in vitro and in vivo and its possible mechanisms of action. We also determined whether there were toxic and side effects during the antitumor process. Our results showed that SFP can inhibit the growth of lung cancer cells both

[1]Department of Clinical Pharmacology, Tianjin Medical University Cancer Institute and Hospital, National Clinical Research Center for Cancer, Key Laboratory of Cancer Prevention and Therapy, Tianjin's Clinical Research Center for Cancer, Tianjin 300060, China and [2]Institute of Biomechanics and Medical Engineering, Tsinghua University, Beijing 100084, China
Correspondence: Zhao Yan (yanzhaopaper@163.com) or Hong-ping Zhao (zhaohp@mail.tsinghua.edu.cn)
These authors contributed equally: Mei-sa Wang, Yi-bo Du.

Anticancer effect of silk fibroin peptide in human lung cancer cells
MS Wang et al.

523

in vitro and in vivo at the present concentrations by inducing cell cycle arrest at the S phase and then promoting the apoptosis of lung cancer cells. Western blot results further showed that SFP could downregulate Bcl-2 protein expression and upregulate Bax protein expression during cell apoptosis.

MATERIALS AND METHODS

Cell lines and culture conditions
Human lung cancer cell lines (A549 and H460) were obtained from the American Type Culture Collection (Manassas, VA, USA). BEAS-2b cells were frozen and stored in our laboratory. All cells, except for BEAS-2b cells, were cultured in Roswell Park Memorial Institute 1640 (Gibco, NY, USA) media supplemented with 10% fetal bovine serum (Gibco, NY, USA), 1% penicillin (100 IU/mL) (Solarbio, Beijing, China), and streptomycin (100 mg/mL) (Solarbio, Beijing, China) at 37 °C in an incubator with a 5% CO_2 atmosphere. BEAS-2b cells were cultured in LHC-8 medium (Gibco, NY, USA).

Drug
SFP with a purity of 98.1% was extracted from SF by Dr. Hong-ping Zhao at Tsinghua University. Extracted peptides were stored at 4 °C and diluted in 1640 medium before use.

Toxicological testing
Toxicological studies were performed on 48 BALB/c mice (half male and half female) weighing ~18–22 g. Mice were obtained from Beijing Vital River Laboratory Animal Technology Co, Ltd (Beijing, China). Mice were treated with vehicle, 15,000 mg/kg SFP and 30,000 mg/kg SFP via intragastric administration for 14 days. Changes in body weight and blood examinations were recorded during treatment. The experimental design of this study was approved by the Animal Care Committee of Tianjin Medical University Cancer Institute and Hospital.

Cell viability assay
The effects of SFP on cellular proliferation and viability were determined using the 3-(4,5-Dimethyl-2-thiazolyl)-2,5-diphenyl-2H-tetrazolium bromide (MTT) assay (R&D Systems, UK). All cells were seeded in 96-well plates at a density of 3.0×10^3 cells/well in 100 μL of medium and allowed to attach overnight. Cells were then treated with SFP at increasing concentrations (0, 3.75, 7.5, 15, 30, 60, and 120 mg/mL) for 24, 48, and 72 h. Subsequently, cells were incubated with the MTT reagent (Beyotime Biotechnology, Shanghai, China) at a final concentration of 5 mg/mL for 4 h. Finally, intracellular formazan crystals were solubilized with 150 μL dimethyl sulfoxide (BEAS-2b cells used LHC-8). The absorbance was measured at 490 nm using an enzyme-linked immunosorbent assay plate reader (Thermo Fisher Scientific, Waltham, MA, USA). Reductions in cell viability in the different treatment groups were expressed as the percentage of viable cells in the treated cells relative to the control cells. All experiments were performed three times.

Colony formation assay
A colony formation assay was performed to evaluate the long-term drug efficiency of SFP. A549 and H460 cells were seeded in 12-well plates at a density of 200 cells/well and allowed to attach overnight. Cells were then exposed to increasing concentrations of SFP (0, 3.75, 7.5, 15, and 30 mg/mL) for 72 h. Next, the culture medium was replaced with fresh medium and incubated for 2 weeks at 37 °C. Cells were then fixed with 100% ethanol (4 °C, 20 min) and stained with 1% crystal violet (Sigma-Aldrich, St Louis, MO, USA) for 15 min. Colonies with > 50 cells were counted. The clonogenic capability was calculated as the ratio between the number of clones in the treated cells and the corresponding number of clones in the control cells. Each experiment was performed three times.

Cell cycle analysis
A cell cycle distribution assay was performed as previously described [20]. In brief, cells were treated with SFP (0, 5, 10, 15, and 20 mg/mL) for 48 h. After treatment, attached cells were trypsinized, harvested, and washed with phosphate-buffered saline (PBS). Cells were centrifuged (1000 r/min, 5 min) and subsequently fixed with ice-cold 70% ethanol for 24 h. After centrifugation, cells were washed twice and resuspended in PBS containing propidium iodide (40 μg/mL), RNase A (100 μg/mL), and Triton X-100 (0.05%) (Beyotime Biotechnology, Shanghai, China) and incubated at 37 °C for 15 min. Cell cycle distribution was analyzed using a FACSCantoII flow cytometer (BD Biosciences, CA, USA). Each experiment was performed three times.

Cell apoptosis analysis
A cell apoptosis assay was performed as previously described [21]. In brief, cells were treated with varying concentrations of SFP (0, 10, 20, 30, 40, and 50 mg/mL) for 48 h. After treatment, cells were washed twice with 1 × binding buffer and labeled with Annexin V and propidium iodide (PI) following the manufacturer's instructions. The cell apoptosis assay was performed using the Apoptosis Analysis Kit (Sigma-Aldrich, St Louis, MO, USA), and apoptosis was analyzed using FACS flow cytometer. Each experiment was performed three times.

Western blotting
Western blotting was performed to determine the changes in protein expression in response to treatment with SFP. Proteins from the treated cell lysates were prepared via Bradford assay. The protein concentration was determined using the Pierce BCA protein assay kit (Thermo Scientific). Equivalent amounts (50 μg of
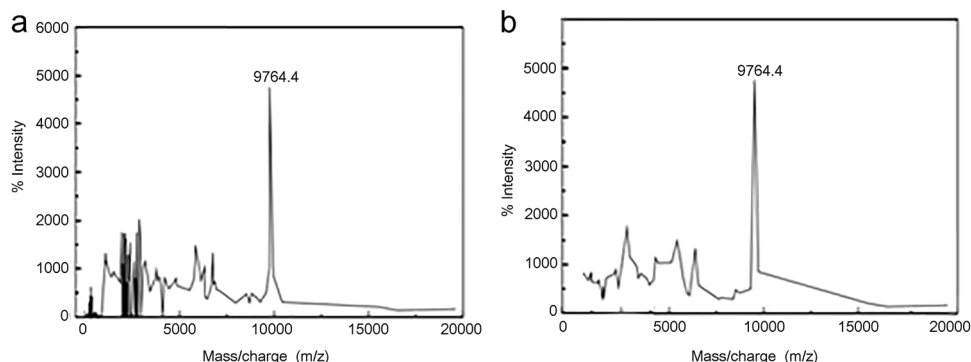

Fig. 1 Molecular weight and amino-acid composition of SFP. **a** Mass spectrogram of the SFP solution before dialysis. **b** Mass spectrogram result of the SFP solution after dialysis with a molecular weight cutoff of 8 kDa

Anticancer effect of silk fibroin peptide in human lung cancer cells
MS Wang et al.

524

protein/lane) of protein were separated via 8% sodium dodecyl sulfate-polyacrylamide gel electrophoresis and transferred onto polyvinylidene membranes by submerging in a transfer tank (Bio-Rad Laboratories). Membranes were blocked for 1 h at room temperature (25 °C) in 5% (w/v) fat-free milk powder in 1 × Tris-buffered saline (TBS) containing 1% Tween 20. Membranes were then incubated with the primary antibodies (1:1000 dilution) with gentle agitation at 4 °C overnight. The primary antibodies were as follows: anti-Bcl-2 (1:1000 dilution, rabbit monoclonal antibody, Cell Signaling Technology, Beverly, USA), anti-β-actin (1:1000 dilution, mouse monoclonal antibody, Cell Signaling Technology, Beverly, USA), and anti-Bax (1:1000 dilution, rabbit monoclonal antibody, Cell Signaling Technology, Beverly, USA). Then, the membranes were washed three times with 0.1% Tween 20 in Tris-HCl buffer and incubated with secondary goat anti-mouse-horseradish peroxidase (HRP) and goat anti-rabbit HRP antibodies (Bio-Rad) at 1:5000 dilutions for 1 h at room temperature. After a final wash with 0.1% Tween 20 in TBS (three times for 10 min each), the blots were developed using a luminescent image analyzer LAS-4000 (Fujifilm, Dielsdorf, Switzerland) and Multi Gauge software (Fujifilm Version 3.0). Each experiment was performed three times.

Tumor xenografts

The assessment of antitumor activity was performed using 5-week-old female BALB/c mice weighing ~ 20 g. In brief, 150 µL of H460 cell suspension (2×10^7 cells/mL) was injected into the right

Is this the sequence??

Table 2. Amino-acid analysis results of SFP

Name	Concentration of silk fibroin peptide before dialysis (µg/mL)	The content (%)	Concentration of silk fibroin peptide after dialysis (µg/mL)	The content (%)
Gly	176.9	30.45	110.6	29.17
Cys	167.1	28.76	95.0	25.06
ALa	63.4	10.90	25.0	6.59
Ser	51.6	8.89	35.1	9.26
Glu	24.7	4.25	22.2	5.86
Asp	18.1	3.11	14.4	3.80
Pro	17.6	3.04	188	4.96
Val	12.2	2.10	9.4	2.48
Arg	11.8	2.04	12.9	3.40
Thr	7.8	1.34	5.9	1.56
Lys	7.5	1.29	6.9	1.82
Leu	6.1	1.04	5.7	1.50
Tyr	5.9	1.03	6.8	1.79
Ile	3.9	0.68	3.6	0.95
Phe	3.5	0.60	4	1.06
His	1.4	0.25	1.4	0.37
Met	1.3	0.24	1.4	0.37
Total	580.8	100.00	379.1	100.00

Table 1. The statistical results of the molecular weight and concentration of SFP before and after dialysis

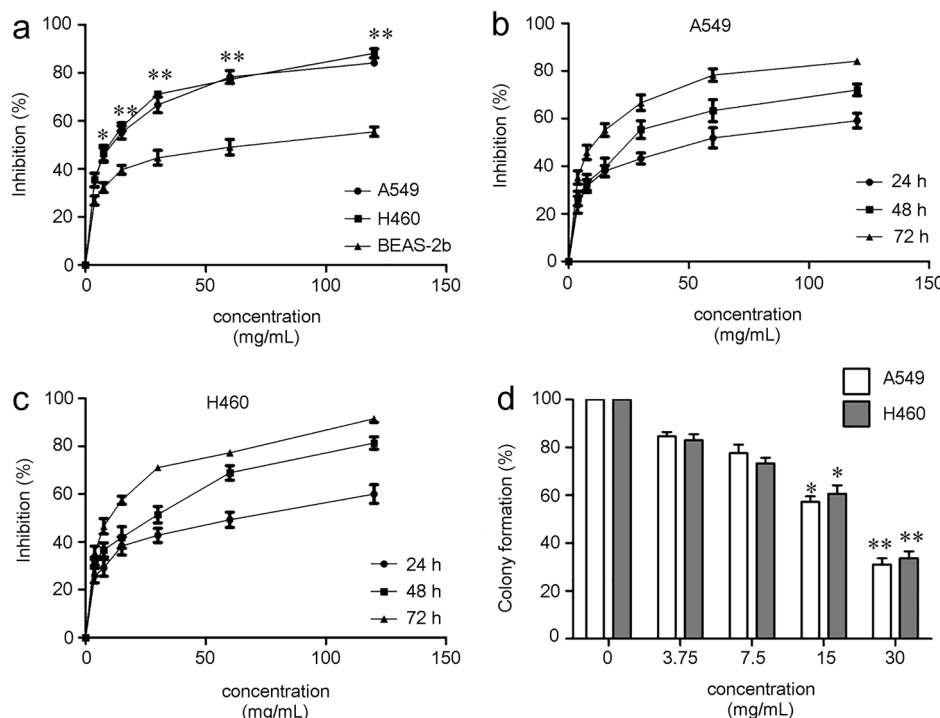| Molecular weight	0–3 kDa	3–5 kDa	5-8 kDa	8–10 kDa	>10 kDa
Content (before dialysis)%	16.6	15.2	18.6	16.6	33.0
Content (after dialysis)%	3.1	10.2	13	16	57.7

Fig. 2 Antiproliferative effects of SFP on lung cancer cells and normal lung epithelial cells in vitro. **a** A549, H460, and BEAS-2b cells treated with varying concentrations (0–120 mg/mL) of SFP for 72 h. Cell viability was analyzed via MTT assay. **b**, **c** A549 and H460 cells treated with varying concentrations (0–120 mg/mL) of SFP for different incubation periods. **d** Colony formation assays of the A549 and H460 cells treated with SFP at the indicated concentrations. Mean ± SD. $n = 3$ **$P < 0.01$, *$P < 0.05$ vs control

Anticancer effect of silk fibroin peptide in human lung cancer cells
MS Wang et al.

525

groin of each mouse. The tumor volume was calculated based on the formula $V = (a \times b^2)/2$ [22], where a represents the length and b represents the width of the tumor. When the tumor volumes reached approximately 100–150 mm³, mice were randomly divided into four groups, the SFP treatment (200 and 500 mg/kg body weight), cisplatin treatment, and control groups, with five mice per group. Mice in the SFP treatment group were intraperitoneally injected with increasing doses of SFP (200 and 500 mg/kg body weight) for 40 days. Mice in the cisplatin treatment group received an intraperitoneal injection of cisplatin at 4 mg/kg twice a week. The tumor volume was measured every 2 days, and body weights were measured daily. The above experiment was repeated using intragastric administration as the route of administration for 21 days using the same treatment groups and doses. SFP was administered via the intragastric route and cisplatin was administered via intraperitoneal injection. At the end of drug treatment, photos were taken of the removed tumor blocks. The experimental design of this study was approved by the Animal Care Committee of Tianjin Medical University Cancer Institute and Hospital.

Statistical analysis

Data were expressed as the mean ± standard error. Statistical analyses were performed using SPSS version 20.0 software. Statistical differences were calculated using the unpaired two-tailed Student's t test. $P \leq 0.05$ was considered statistically significant.

RESULTS

Extraction of SFP

SFP was dissolved in ethanol–CaCl₂ solution. Desalination and concentration were performed via dialysis. The silkworm extract was prepared at a concentration of 1:25 (m/v) with boiled distilled water containing 0.25% Na₂CO₃ and was subsequently incubated in a boiling water bath for 1 h. Then, the resulting solution was added to the ternary solution (CaCl₂:H₂O:C₂H₅OH = 1:7:2) at a concentration of 1:20 (m/v) and incubated at room temperature for 1 h. Next, the solution was incubated at 60 °C in a water bath and allowed to dissolve for 1 h to a final concentration of 1:10 (m/v). After complete dissolution, the mixture was centrifuged at 1000 r/min for 30 min, after which the supernatant was isolated
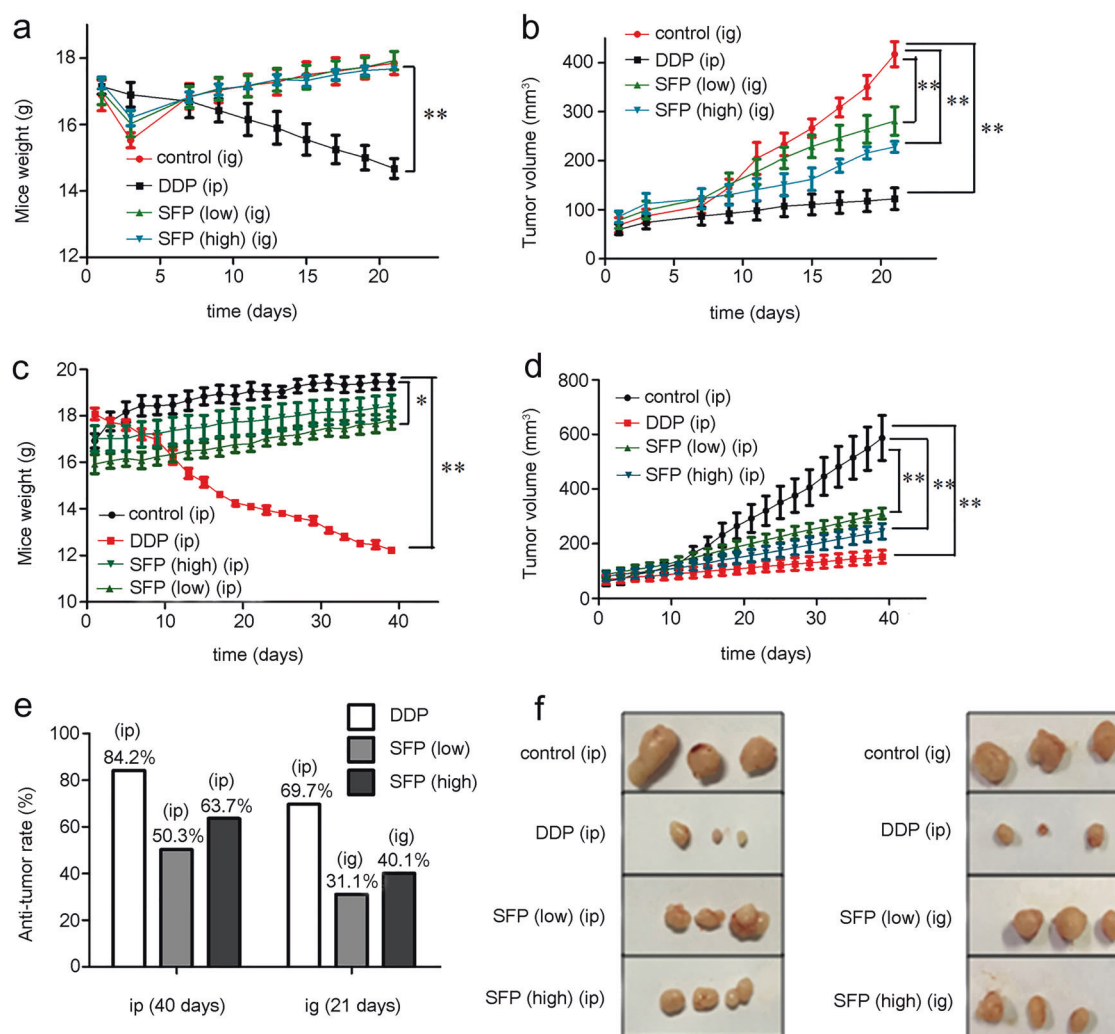

Fig. 3 **a**, **b** Tumor-bearing mice were treated with vehicle, SFP (200 and 500 mg/kg), or cisplatin for 21 days. Vehicle was administered via intragastrically in the control group. SFP was administered via intragastrically in the SFP group. Cisplatin was administered via intraperitoneal injection. The body weights **a** and tumor growth rates **b** were measured as described in the Materials and Methods section. **c**, **d** Tumor-bearing mice were intraperitoneally injected with vehicle, SFP (200 and 500 mg/kg), and cisplatin for 40 days. Body weights **c** and tumor growth rates **d** were measured as described in the Materials and Methods. **e** The anticancer ratio of the two routes of administration. **f** Antitumor effect of SFP in vivo. BALB/c (nude) mice were administered normal saline, DDP, low-dose SFP (200 mg/kg), and high-dose SFP (500 mg/kg). Photos of tumors were taken after the end of drug administration. Mean ± SD. $n = 5$ **$P < 0.01$, *$P < 0.05$ vs control

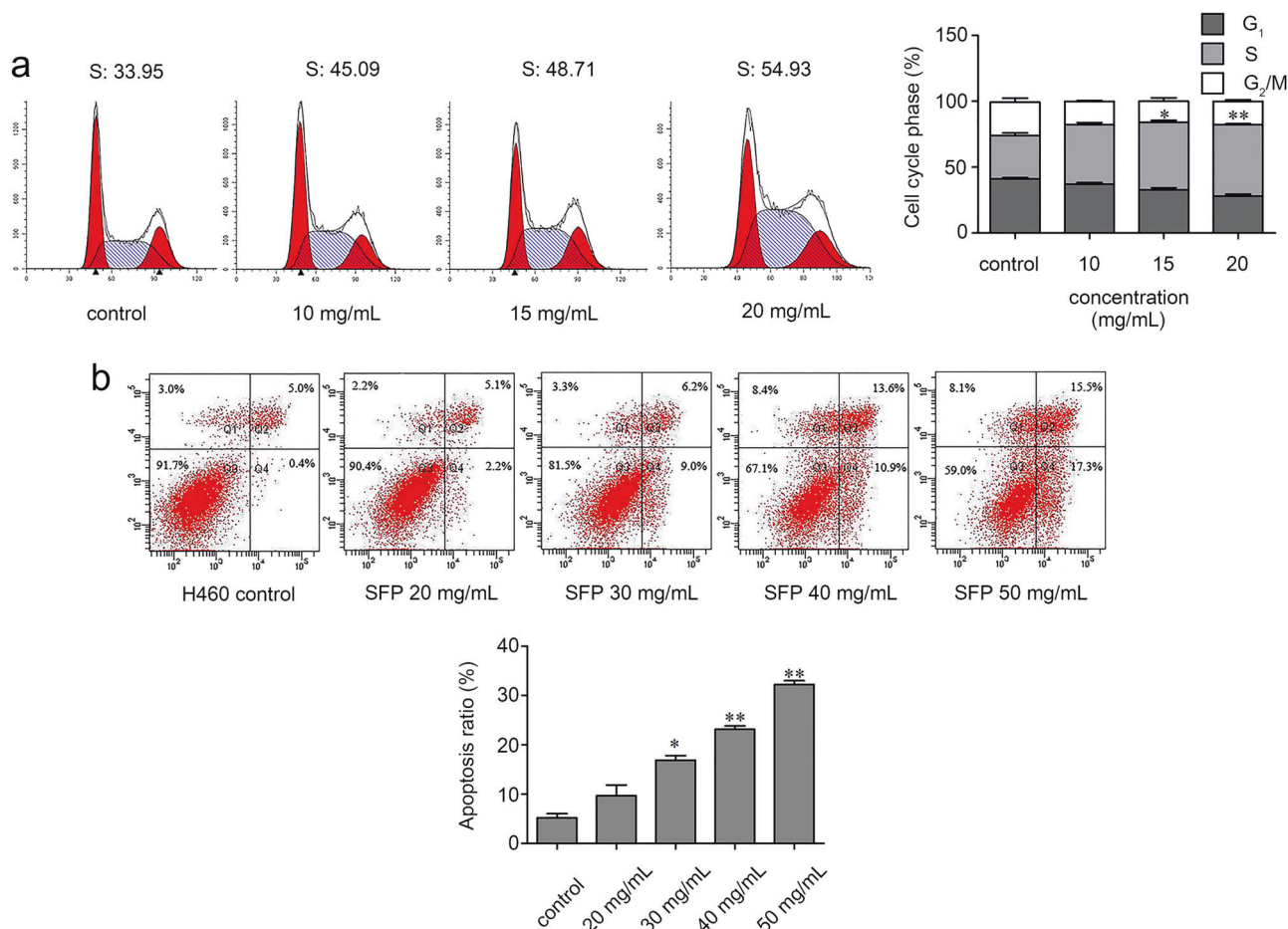Anticancer effect of silk fibroin peptide in human lung cancer cells
MS Wang et al.

526

Fig. 4 SFP triggers cell cycle arrest at the S phase and regulates apoptosis in H460 cells. **a, b** H460 cells were treated with various concentrations of SFP for 48 h. Cell cycle distribution **a** and cell apoptosis **b** were analyzed using Verity's Modfit LT 3. 0 software. Mean ± SD. n = 3 **$P < 0.01$, *$P < 0.05$ vs control

and incubated at 4 °C. The molecular weight and amino-acid composition of the SFP were determined via mass spectrometry and amino-acid analysis. The results showed that SFP yielded a maximum peak at ~ 10 kDa (Fig. 1a). Statistical analysis of the molecular weights of the SFP before dialysis showed that molecules with weights higher than 8 kDa accounted for almost half of the total sample (Table 1). Dialysis of the SFP was performed using a dialysis bag with a molecular weight cutoff of 8 kDa. A maximum peak was located at ~ 10 kDa (Fig. 1b), and statistical analysis of the molecular weight of SFP before dialysis showed that molecules with weights greater than 8 kDa accounted for 60% of the total sample (Table 1). Taken together, the above results showed that the molecular weight of SFP is ~ 10 kDa. The dominant amino acids present in SFP were glycine, cysteine, alanine, and serine, which together accounted for 70.1% (before dialysis) and 79.0% (after dialysis) of the total weights of the amino acids. Moreover, glycine showed the highest content with ~ 30.45% (before dialysis) and 29.17% (after dialysis) (Table 2).

Safety evaluation of SFP
For each treatment group, the initial mouse weights were low and increased. The low initial weight was due to the abrosia before intragastric administration. After 2 days, all groups showed increasing weights (Supplementary Figure 1a and b). The results showed no significant effect of the treatments on mouse weight. After treatment, blood was collected for the measurement of routine blood parameters and biochemistry indicators. The results showed that both routine blood parameters (Supplementary

Table 1) and blood biochemistry (Supplementary Table 2) parameters were within the normal range of fluctuations.

SFP inhibits the proliferation of lung cancer cells in vitro and in vivo
To explore the anticancer effects of SFP both in vitro and in vivo, we first examined the inhibitory effects of SFP on human lung cancer cell lines and normal lung epithelial cells (Beas-2b). SFP displayed moderate cytotoxicity to BEAS-2b cells with an inhibitory concentration (IC_{50}) of 81.54 mg/mL determined via MTT assay (Fig. 2a). However, the IC_{50} of SFP in A549 cells was 9.921 mg/mL, which was significantly lower than in BEAS-2b cells. In another lung cancer cell line, H460, the IC_{50} of SFP was 9.083 mg/mL, which was also lower than that in BEAS-2b cells (Fig. 2b). The results of the MTT assay showed that SFP inhibited the proliferation of lung cancer cells in a dose-dependent manner (Fig. 2c). SFP also suppressed the clonogenic activity of these two cell lines (Fig. 2d). We also studied the IC_{50} of SFP on several other tumor cell lines (Supplementary Table 3).

In the treatment group, H460 cells were implanted in BALB/c (nude) mice via subcutaneous injection. For the positive control, BALB/c (nude) mice were injected with cisplatin [23]. Growth of the implanted tumors was significantly inhibited in the cisplatin group; however, the body weights of the cisplatin-mice decreased rapidly. By contrast, we observed no significant changes in the weights of mice in the control and SFP groups (Fig. 3a). After the drug treatment ended, we killed the nude mice and photographed the removed tumor blocks. SFP significantly inhibited the
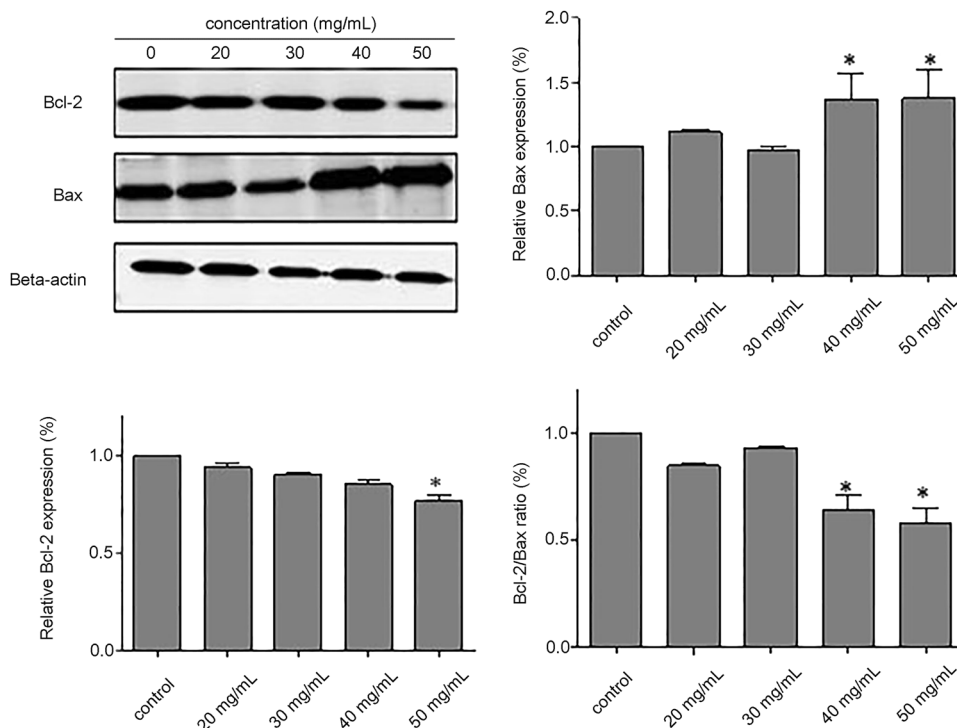
Anticancer effect of silk fibroin peptide in human lung cancer cells
MS Wang et al.

527

Fig. 5 H460 cells were incubated with various concentrations of SFP for 48 h. Bax and Bcl-2 protein expression levels were detected via western blotting using β-actin as internal control. **$P < 0.01$, *$P < 0.05$ vs control

growth of the implanted tumors. The tumor growth inhibition by SFP in the high-dose group was more pronounced than in the low-dose group but less pronounced than in the cisplatin group (Fig. 3b). Although cisplatin showed a strong tumor inhibitory effect in H460 tumor-bearing mice, the drug exhibited very high toxicity, whereas SFP showed almost no toxicity during treatment. The above experiment was then repeated using intraperitoneal injection as the route of administration, and the treatment period was prolonged to 40 days. The results for the intraperitoneal injection showed similar results to those obtained using intragastric administration. Cisplatin treatment significantly decreased the body weights of mice. However, SFP did not induce significant changes in body weights even after 40 days of treatment (Fig. 3c). Furthermore, SFP showed more pronounced anticancer effects with little toxicity in a dose-dependent manner compared with cisplatin (Fig. 3d). In addition, we found no significant differences in tumor inhibition rates between the two routes of administration (Fig. 3e). We could clearly see changes in the tumor block after the administration of the drug (Fig. 3f). The above results demonstrated that SFP effectively inhibited the proliferation of human lung cancer cells. Moreover, SFP showed lower toxicity both in vitro and in vivo.

SFP regulates the cell cycle and cell apoptosis
First, we evaluated the effects of SFP on the cell cycle distribution. H460 cells treated with or without SFP were subjected to flow cytometry analysis. The results showed that cells treated with SFP showed a higher proportion of cells in the S phase compared with control samples (Fig. 4a). SFP-induced cell cycle arrest at the S phase in a concentration-dependent manner.

The extent of apoptosis was determined via flow cytometry using Annexin V-FITC/PI staining. The results showed that after treating H460 cells for 48 h, the apoptosis rate increased from ~5.1–32.8% with increasing concentrations of SFP (Fig. 4b). The results indicated that SFP-induced cell apoptosis in a concentration-dependent manner.

Apoptosis is regulated by multiple proteins, including Bcl-2 family members [24]. To determine whether apoptosis-related proteins are involved in regulating SFP-induced apoptosis, we examined the protein levels of Bcl-2 and Bax in H460 cells (Fig. 5). The results indicated that SFP treatment significantly down-regulated the expression of the anti-apoptosis protein Bcl-2 and upregulated the expression of the pro-apoptotic protein Bax in a dose-dependent manner.

DISCUSSION

SF was previously reported to suppress tumorigenesis both in vivo and in vitro [13]. However, only a limited number of studies investigated the anticancer activity of SFP and the possible mechanisms underlying its effects. Thus, we investigated the anticancer activity of SFP and elucidated the potential molecular mechanisms underlying its effects. Our results showed that SFP effectively inhibited the growth of lung cancer cells both in vitro and in vivo, with the concomitant induction of cell cycle arrest and apoptosis. Furthermore, SFP did not show significant toxicity to normal lung cells and normal mice. These results suggested that SFP selectivity affects cancer cells and not normal cells, which can be attributed to differences in genomic stability between cancer and normal cells [25].

Our findings demonstrated that SFP is highly safe for use in the normal body. After 14 days of treatment, SFP increased body weights and did not affect the vital signs of mice. No obvious changes were observed for routine blood parameters and blood biochemical parameters in the treatment group compared with the control group. Body weights, vital signs, routine blood parameters, and blood biochemical parameters are the standard evaluation indices in animal toxicity experiments [26], and all results indicated that SFP is highly safe for animals. Thus, SFP can be used for the clinical treatment of lung cancer without inducing adverse reactions and reducing the pain caused by adverse reactions in patients.

528

SFP effectively inhibited the proliferation of lung cancer cells both in vitro and in vivo. Surprisingly, the two different modes of administration did not induce significant differences in the parameters tested. Therefore, we hypothesized that fibroin peptides escaped degradation in the gastrointestinal system because of their small molecular weights. The anticancer effects of SFP showed a close association with the cell cycle [27] and cell apoptosis [28, 29]. The cell cycle is the process that maintains the life of the cell and is divided into four consecutive stages, the G_1, S, G_2, and M phases [30]. The cell cycle is primarily regulated by three types of proteins, cyclin, CDK, and CDKI [31], which are involved in DNA synthesis and cell division. Changes in the activity of cyclin, CDK, and CDKI may disrupt cell proliferation, which can, in turn, lead to cancer [32]. In the present study, SFP induced an increase in the distribution of cells in the S phase, indicating cell cycle arrest of the lung cancer cell cycle in the DNA synthesis phase of the cell cycle [33]. The results revealed that SFP can influence the DNA synthesis of lung cancer cells. Cell apoptosis or programmed cell death is the primary mechanism by which chemotherapeutic drugs inhibit the growth of cancer cells [34]. Apoptosis is mediated by two signaling pathways: the intrinsic pathway, which involves the activation of mitochondria and several caspases, and the extrinsic pathway, which involves the activation of death receptors [35]. The Bcl-2 family of proteins are associated with the mitochondrial pathway [36, 37] and consists of two types of proteins: Bax, which promotes apoptosis, and Bcl-2, which inhibits apoptosis [38]. Our results showed that SFP can induce apoptosis in H460 cells in a concentration-dependent manner. H460 cells treated with SFP showed upregulation of Bax and downregulation of Bcl-2. These findings suggested that SFP can promote cell apoptosis via the mitochondrial pathway. However, further experiments must be conducted to examine the changes in expression of other key proteins involved in the mitochondrial pathway.

In conclusion, our findings showed that SFP extracted from silk cocoons has antiproliferative effects on lung cancer cells both in vivo and in vitro. SFP exerts its anticancer effects by inducing cell cycle arrest in the S phase and regulating the activity of Bcl-2 and Bax proteins to induce the apoptosis of lung cancer cells. Furthermore, SFP showed no cytotoxic effects in mice and thus does not affect the animal life status. Therefore, SFP is a promising therapeutic agent for the clinical treatment of lung cancer and does not induce toxicity and adverse side effects.

AUTHOR CONTRIBUTION
Zhao Yan, Hong-ping Zhao, Zhong-ling Zhu, and Mei-sa Wang designed the research; Mei-sa Wang, Yi-bo Du, Hui-ming Huang, Shuang-shuang Du, and Shao-yong Chen performed the research; Mei-sa Wang and Yi-bo Du analyzed the data.

ADDITIONAL INFORMATION
The online version of this article (https://doi.org/10.1038/s41401-018-0048-0) contains supplementary material, which is available to authorized users.

Competing interests: The authors declare that there are no conflicts of interest.

REFERENCES
1. Wu XY, Huang XE. Screening for patients with non-small cell lung cancer who could survive long term chemotherapy. Asian Pac J Cancer Prev. 2015;16:647–52.
2. Yang J, Zhu J, Zhang YH, Chen YS, Ding LL, Kensler TW, et al. Lung cancer in a rural area of China: rapid rise in incidence and poor improvement in survival. Asian Pac J Cancer Prev. 2015;16:7295–302.
3. de Oliveira VA, Da ML, De Bastiani MA, Lopes FM, Muller CB, Gabiatti BP, et al. In vitro evaluation of antitumoral efficacy of catalase in combination with traditional chemotherapeutic drugs against human lung adenocarcinoma cells. Tumour Biol. 2016;37:10775–84.
4. Shen J, Ma H, Zhang T, Liu H, Yu L, Li G, et al. Magnolol inhibits the growth of non-small cell lung cancer via Inhibiting microtubule polymerization. Cell Physiol Biochem. 2017;42:1789–801.
5. Lei JP, Yuan JJ, Pi SH, Wang R, Tan R, Ma CY, et al. Flavones and lignans from the stems of wikstroemia scytophylla Diels. Pharmacogn Mag. 2017;13:488–91.
6. Aramwit P, Siritientong T, Srichana T. Potential applications of silk sericin, a natural protein from textile industry by-products. Waste Manag Res. 2012;30:217–24.
7. Kunz Rl, Brancalhao RM, Ribeiro LF, Natali MR. Silkworm sericin: properties and biomedical applications. Biomed Res Int. 2016;2016:8175701.
8. Yerra A, Mysarla DK, Siripurapu P, Jha A, Valluri SV, Mamillapalli A. Effect of polyamines on mechanical and structural properties of Bombyx mori silk. Biopolymers. 2017;107:20–27.
9. Du S, Zhang J, Zhou WT, Li QX, Greene GW, Zhu HJ, et al. Interactions between fibroin and sericin proteins from Antheraea pernyi and Bombyx mori silk fibers. J Colloid Interface Sci. 2016;478:316–23.
10. Unajak S, Aroonluke S, Promboon A. An active recombinant cocoonase from the silkworm Bombyx mori: bleaching, degumming and sericin degrading activities. J Sci Food Agric. 2015;95:1179–89.
11. Kato N, Sato S, Yamanaka A, Yamada H, Fuwa N, Nomura M. Silk protein, sericin, inhibits lipid peroxidation and tyrosinase activity. Biosci Biotechnol Biochem. 1998;62:145–7.
12. Zhaorigetu S, Sasaki M, Watanabe H, Kato N. Supplemental silk protein, sericin, suppresses colon tumorigenesis in 1,2-dimethylhydrazine-treated mice by reducing oxidative stress and cell proliferation. Biosci Biotechnol Biochem. 2001;65:2181–6.
13. Kaewkorn W, Limpeanchob N, Tiyaboonchai W, Pongcharoen S, Sutheer-awattananonda M. Effects of silk sericin on the proliferation and apoptosis of colon cancer cells. Biol Res. 2012;45:45–50.
14. Totten JD, Wongpinyochit T, Seib FP. Silk nanoparticles: proof of lysosomotropic anticancer drug delivery at single-cell resolution. J Drug Target. 2017;25:865–72.
15. Gupta V, Aseh A, Rios CN, Aggarwal BB, Mathur AB. Fabrication and characterization of silk fibroin-derived curcumin nanoparticles for cancer therapy. Int J Nanomed. 2009;4:115–22.
16. Prateep A, Sumkhemthong S, Suksomtip M, Chanvorachote P, Chaotham C. Peptides extracted from edible mushroom: lentinus squarrosulus induces apoptosis in human lung cancer cells. Pharm Biol. 2017;55:1792–9.
17. Cao QZ, Lin ZB. Ganoderma lucidum polysaccharides peptide inhibits the growth of vascular endothelial cell and the induction of VEGF in human lung cancer cell. Life Sci. 2006;78:1457–63.
18. Oroz-Parra I, Navarro M, Cervantes-Luevano KE, Alvarez-Delgado C, Salvesen G, Sanchez-Campos LN, et al. Apoptosis activation in human lung cancer cell lines by a novel synthetic peptide derived from conus californicus venom. Toxins (Basel). 2016;8:38.
19. Mcconnell EJ, Devapatla B, Yaddanapudi K, Davis KR. The soybean-derived peptide lunasin inhibits non-small cell lung cancer cell proliferation by suppressing phosphorylation of the retinoblastoma protein. Oncotarget. 2015;6:4649–62.
20. Welschinger R, Bendall LJ. Temporal tracking of cell cycle progression using flow cytometry without the need for synchronization. J Vis Exp 2015;16:e52840.
21. Zhu Y, He W, Gao X, Li B, Mei C, Xu R, et al. Resveratrol overcomes gefitinib resistance by increasing the intracellular gefitinib concentration and triggering apoptosis, autophagy and senescence in PC9/G NSCLC cells. Sci Rep. 2015;5:17730.
22. Yan Z, Zhu Z, Wang J, Sun J, Chen Y, Yang G, et al. Synthesis, characterization, and evaluation of a novel inhibitor of WNT/beta-catenin signaling pathway. Mol Cancer. 2013;12:116.
23. Ding F, Wang M, Du Y, Du S, Zhu Z, Yan Z. BHX inhibits the Wnt signaling pathway by suppressing beta-catenin transcription in the nucleus. Sci Rep. 2016;6:38331.
24. Liu C, Gong K, Mao X, Li W. Tetrandrine induces apoptosis by activating reactive oxygen species and repressing Akt activity in human hepatocellular carcinoma. Int J Cancer. 2011;129:1519–31.
25. Yang CH, Craise LM. Development of human epithelial cell systems for radiation risk assessment. Adv Space Res. 1994;14:115–20.
26. Zbinden G, Kleinert R, Rageth B. Assessment of emetine cardiotoxicity in a subacute toxicity experiment in rats. J Cardiovasc Pharmacol. 1980;2:155–64.
27. Sa G, Das T. Anti cancer effects of curcumin: cycle of life and death. Cell Div. 2008;3:14.

Anticancer effect of silk fibroin peptide in human lung cancer cells
MS Wang et al.

529

28. Lian Z, Niwa K, Gao J, Tagami K, Mori H, Tamaya T. Association of cellular apoptosis with anti-tumor effects of the Chinese herbal complex in endocrine-resistant cancer cell line. Cancer Detect Prev. 2003;27:147–54.

29. Sun W, Wang W, Kim J, Keng P, Yang S, Zhang H, et al. Anti-cancer effect of resveratrol is associated with induction of apoptosis via a mitochondrial pathway alignment. Adv Exp Med Biol. 2008;614:179–86.

30. Russo LC, Araujo CB, Iwai LK, Ferro ES, Forti FL. A Cyclin D2-derived peptide acts on specific cell cycle phases by activating ERK1/2 to cause the death of breast cancer cells. J Proteom. 2017;151:24–32.

31. Tyagi A, Agarwal C, Harrison G, Glode LM, Agarwal R. Silibinin causes cell cycle arrest and apoptosis in human bladder transitional cell carcinoma cells by regulating CDKI-CDK-cyclin cascade, and caspase 3 and PARP cleavages. Carcinogenesis. 2004;25:1711–20.

32. Thakur R, Kini S, Kurkalang S, Banerjee A, Chatterjee P, Chanda A, et al. Mechanism of apoptosis induction in human breast cancer MCF-7 cell by Ruviprase, a small peptide from Daboia russelii russelii venom. Chem Biol Interact. 2016;258:297–304.

33. Li D, Dai C, Yang X, Li B, Xiao X, Tang S GADD45a Regulates olaquindox-induced DNA damage and S-phase arrest in human hepatoma G2 cells via JNK/p38 pathways. Molecules 2017; 22: pii: E124.

34. Adams JM. Therapeutic potential of a peptide targeting BCL-2 cell guardians in cancer. J Clin Invest. 2012;122:1965–7.

35. Elmore S. Apoptosis: a review of programmed cell death. Toxicol Pathol. 2007;35:495–516.

36. Zou Y, Li Q, Jiang L, Guo C, Li Y, Yu Y, et al. DNA hypermethylation of CREB3L1 and Bcl-2 associated with the mitochondrial-mediated apoptosis via PI3K/Akt pathway in human BEAS-2B cells exposure to silica nanoparticles. PLoS ONE. 2016;11:e0158475.

37. Liu D, Yi B, Liao Z, Tang L, Yin D, Zeng S, et al. 14-3-3gamma protein attenuates lipopolysaccharide-induced cardiomyocytes injury through the Bcl-2 family/mitochondria pathway. Int Immunopharmacol. 2014;21:509–15.

38. Siddiqui WA, Ahad A, Ahsan H. The mystery of BCL2 family: Bcl-2 proteins and apoptosis: an update. Arch Toxicol. 2015;89:289–317.